redin Revista Facultad de Ingeniería, Universidad de Antioquia, No.93, pp. 32-40, Oct-Dec 2019

Doppler spectrum measurements of vehicular radio channels using a narrowband sounder

Mediciones de espectro Doppler de canales de radio vehicular usando un sondeador de banda angosta

Carlos A. Gómez-Vega [1], **Carlos A. Gutiérrez** [1*], **José J. Jaime-Rodríguez** [2], **Javier Vázquez Castillo** [3], **Daniel U. Campos-Delgado** [1], **José M. Luna-Rivera** [1], **Miguel A. Díaz-Ibarra** [1]

[1]Facultad de Ciencias, Universidad Autónoma de San Luis Potosí. Av. Chapultepec 1570, Privadas del Pedregal. C. P. 78295. San Luis Potosí, México.
[2]Unidad Académica Multidisciplinaria Zona Media, Universidad Autónoma de San Luis Potosí. Carretera Rioverde-San Ciro Km 4, El Carmen. C. P. 79615. San Luis Potosí, México.
[3]División de Ciencias e Ingeniería, Universidad de Quintana Roo. Boulevard Bahía s/n esq. Ignacio Comonfort, Col. del Bosque. C. P. 77019. Quintana Roo, México.

CITE THIS ARTICLE AS:

C. A. Gómez-Vega and *et al*, "Doppler spectrum measurements of vehicular radio channels using a narrowband sounder", *Revista Facultad de Ingeniería Universidad de Antioquia*, no. 93, pp. 32-40, Oct-Dec 2019. [Online]. Available: `https://www.doi.org/10.17533/10.17533/udea.redin.20190405`

ARTICLE INFO:

Received: March 20, 2019
Accepted: April 24, 2019
Available online: April 26, 2019

KEYWORDS:

Doppler, measurements, vehicular communications, wireless propagation

Doppler, mediciones, comunicaciones vehiculares, propagación inalámbrica

ABSTRACT: This paper describes the implementation of a narrowband sounder for Doppler power spectrum (DPS) measurements of vehicular communication channels. The narrowband channel sounder is implemented using general purpose equipment, making such measurement platform easy to replicate for didactic and research purposes. To demonstrate the practical value of this framework, a measurement campaign was conducted to obtain empirical information about the spectral characteristics of vehicle-to-vehicle (V2V) and vehicle-to-infrastructure (V2I) multipath radio channels in the 700 MHz band. The collected data were processed to compute the average Doppler shift and the Doppler spread of the measured channels. The obtained results show that the spectral properties of frequency-dispersive vehicular radio channels can be effectively analyzed using narrowband sounding principles.

RESUMEN: Este trabajo describe la implementación de un sondeador de banda angosta para mediciones de espectro de potencia Doppler (EPD) de canales de comunicación vehicular. El sondeador de canal de banda angosta es implementado usando equipo de propósito general, por lo que esta plataforma de medición puede ser reproducida fácilmente para propósitos de docencia e investigación. Para ejemplificar el funcionamiento de la plataforma, se llevó a cabo una campaña de mediciones del EPD de canales de comunicación de vehículo a vehículo (V2V, por sus siglas en inglés) y de vehículo a infraestructura (V2I, por sus siglas en inglés) en la banda de 700 MHz. Los datos recolectados fueron procesados para obtener los momentos estadísticos relevantes del EPD de los canales medidos, es decir, el desplazamiento Doppler promedio y la dispersión Doppler. Los resultados obtenidos muestran que las características espectrales de los canales de comunicación vehicular con dispersión en frecuencia pueden ser investigadas usando principios de sondeo de banda angosta.

1. Introduction

The intelligent transportation systems (ITS) have emerged as a new technology that aims to enhance road safety and traffic flow management. These systems integrate information and communication technologies to assist drivers by means of applications that exploit collaborative networking principles [1, 2]. The capability of exchanging information among vehicles depends on reliable wireless communication links. The dedicated short-range communication (DSRC) is the specific technology that enables vehicle-to-vehicle (V2V) and vehicle-to-infrastructure (V2I) links for safety threat applications [3, 4].

* Corresponding author: Carlos A. Gutiérrez
E-mail: cagutierrez@ieee.org
ISSN 0120-6230
e-ISSN 2422-2844

DOI: 10.17533/10.17533/udea.redin.20190405

Several organizations have been working on the standardization of DSRC technology. For instance, the Institute of Electrical and Electronics Engineers (IEEE) developed an amendment to the IEEE 802.11 standard to address vehicular environments. This amendment, known as IEEE 802.11p standard, sets the guidelines for the physical layer and the medium access control (MAC) sublayer of DSRC systems in the 5.9 GHz band (5.850 GHz – 5.925 GHz) [5]. The IEEE 802.11p standard focuses on this frequency band since regulatory agencies in the US and Europe have allocated this portion of the electromagnetic spectrum for the DSRC technology [3]. In addition to the standardization efforts in the 5.9 GHz spectrum, there is an increasing interest in the 700 MHz band. This frequency is considered in Japan as an alternative for DSRC devices. In this country, the Association of Radio Industries and Business (ARIB) published the ARIB STD-T109 to regulate the requirements of radio frequency (RF) equipment for ITS in the 700 MHz band [6].

In addition to procuring interoperability among DSRC products developed by different manufacturers, the design of transmission schemes for vehicular communication systems must take into account the propagation characteristics of V2V and V2I channels [7, 8]. The wireless channel in vehicular environments is strongly influenced by several factors, such as the high mobility of vehicles, the antenna positioning, and the density of interfering objects (other vehicles, buildings, trees, etc.) [9]. Furthermore, research works have demonstrated that the vehicular channel presents the characteristics of a non-stationary stochastic process [10, 11]. Although the development of theoretical channel models that provide an abstraction of wireless propagation is highly important (e.g. the channel models in [12, 13]), field measurements must be conducted in order to obtain realistic information of the vehicular channel.

Several research works have focused on the vehicular channel characterization through measured data obtained using wideband sounding principles. For instance, the results of a ray tracing simulator are compared with measured data in intersection scenarios in [14]. The authors employed a wideband channel sounder that allows measuring both time and frequency domain characteristics. On the other hand, a programmable testbench that combines vector signal analyzers and vector function generators was implemented in [15]. This architecture was employed to measure the first order statistics (e.g. path-loss, shadowing and small-scale fading distributions) of the wireless channel in the 5.9 GHz band [15]. Concerning the 700 MHz band, a wideband channel sounder was implemented in [16] to obtain the spectral statistical moments and the channel coherence intervals in time and frequency.

The implementation of a wideband channel sounder is a complex task that requires expensive specific purpose equipment which is not available in most universities and research institutes. As an alternative, partial information of the channel characteristics can be obtained employing narrowband sounders built up with general purpose devices. This approach takes advantage of the features of generic RF signal generators, vector network analyzers or spectrum analyzers. The use of narrowband channel sounders has typically been restricted to the analysis of the channel's first order statistics, namely, path-loss and fading (see [17]). However, such equipment can be used as well to measure the spectral properties of frequency-dispersive channels, such as the Doppler power spectrum (DPS). The DPS enables to study the time-varying and non-stationary nature of vehicular channels [12, 13].

In order to facilitate the empirical characterization of frequency-dispersive vehicular radio channels, this paper presents the implementation of a narrowband sounder for DPS measurements. The primary objective of this work is to present a detailed description of a measurement platform constructed with general purpose equipment. This measurement platform is constructed with a commercial off-the-shelf spectrum analyzer and a RF signal generator. Such equipment is commonly available in wireless communications laboratories. This measurement framework is therefore easily replicable, both for didactic and research purposes. To demonstrate the practical value of the narrowband sounder, a measurement campaign was conducted in an urban environment in the city of San Luis Potosí, Mexico, at 700 MHz. The experiments were performed in low mobility conditions in an urban uncontrolled scenario. Nevertheless, these measurements can be replicated in other propagation scenarios following the same framework. Also, the experiments can be extended considering a different carrier frequency (e.g. 5.9 GHz). The measured data were processed to obtain the DPS and its first moment and the square root of the second central moment, i.e. the average Doppler shift and the Doppler spread. The presented results can be used as a reference for the design and evaluation of robust transmission schemes for vehicular communications.

In this paper, we complement our preliminary work presented in [18] by including important details on the implementation of the narrowband channel sounder, as well as, by providing a thorough discussion of the data reduction and processing methodology. Hence, the scope of our previous contribution is expanded here as follows:

1. We complete here a thorough review of the narrowband channel sounding principle that is

exploited in the experimental testbed.

2. We present now technical details of the experimental setup in this paper to complete the description of the measurement platform in [18].

3. We include a new section on the data reduction and processing methodology to elaborate the discussion that was omitted in [18] due to space limitations.

4. Finally, we enhance here the discussion of the obtained results in [18] by providing more technical insight.

The remainder of the paper is organized as follows: A brief review of narrowband channel sounding is presented in Section 2. In Section 3, the implementation of the measurement testbed is described. In Section 4, the methodology for data reduction and processing is presented. The application of the narrowband channel sounder to the measurement of Doppler power spectra of V2V and V2I channels at 700 MHz is discussed in Section 5. Finally, the conclusions are summarized in Section 6.

2. Narrowband channel sounding

In wireless communications, the received signal is a superposition of multiple electromagnetic waves that travel through the channel over different paths. These waves are attenuated, time-delayed and phase-shifted replicas of the original transmitted signal due to the interaction with interfering objects. This form of transmission, known as multipath propagation, causes different problems in communication systems, such as fluctuations on the received signal strength (fading) and intersymbol interference [19]. In addition, as a consequence of multipath propagation and the dynamic behavior of the transmitting and receiving mobile stations, the Doppler effect also affects the communication link. The frequency shifts experienced by the transmitted waves due to the Doppler effect distort the received signal, scattering the received signal's energy in the frequency domain. The Doppler shift experienced by the n-th multipath component is related to the speed of the mobile stations in the direction of the wave propagation [20]. In other words, the angle of arrival (AOA) of the n-th multipath component determines whether the frequency drifts are negative or positive. In a general form, the Doppler shift is positive when the direction of the AOA is contrary to the movement direction, whereas the drift will be negative when the directions of the AOA and the receiving mobile station are the same. On the other hand, the speed of the mobile determines the maximum Doppler shift $f_{\max}$, which is the magnitude of the largest drift that the waves can experience.

The empirical characterization of the propagation impairments requires an appropriate channel sounding method [21]. The basic sounding principle consists of the transmission of a known signal that "excites" the channel. The output of the channel is observed and stored at the receiver for later processing [20]. The received signal has information about the channel response and its eigenvalues. From the knowledge of both transmitted and received signals, the channel behavior can be estimated employing filtering and statistical methods [21].

Channel sounders can be classified as wideband or narrowband. Wideband time-domain sounders are employed to obtain the impulse response of the time-variant vehicular channel. For instance, impulse sounders measure the received signal's echoes by transmitting periodic pulses [20, 21]. This technique allows measuring the complete information of the channel impulse response. Nevertheless, the implementation of the impulse sounder is a difficult task since practical RF components have a finite bandwidth. In addition, an ideal pulse signal cannot be generated in practice. An alternative approach for wideband channel sounding employs correlation principles. These type of sounders exploit the correlation properties of pseudo-noise sequences to obtain the channel impulse response. This technique requires special considerations since the results depend on the properties of the sounding sequence [22]. In general, the implementation of wideband platforms relies on specific purpose RF equipment. Therefore, the sounding platform can only be used to measure the channel response at specific frequency bands.

On the other hand, narrowband sounders are useful to obtain partial characteristics of the channel. These sounders provide information of the signal strength at the transmitted carrier frequency. Narrowband sounders transmit a sinusoidal continuous wave (CW) at a desired frequency (eigenfunction) to measure the received signal strength (eigenvalues). Ideally, in a line-of-sight (LOS) path with static transmitting and receiving stations, an attenuated pure tone will be observed at the transmitted frequency. Nevertheless, due to the motion of the communication stations, this tone will be distorted by the Doppler effect and its energy will be scattered in the frequency domain. This frequency dispersion can be measured using a conventional spectrum analyzer by considering a small observation window in the frequency domain spanning a few hundred of Hertz. This principle is illustrated in Figure 1 by showing the transmitted and received spectra of a sinusoidal CW with frequency f_c. Figure 1a shows the observed received signal when the frequency span of the measurement device (the spectrum analyzer) is set equal to zero. Then, the measured spectrum considering a non zero frequency span is shown in Figure 1b, where multiple power peaks generated by the Doppler shifts of the received multipath signal are observed.

In addition, the narrowband sounding principles can also be employed to construct wideband channel sounders. The sampled spectrum wideband sounding consists of sampling the channel frequency spectrum by transmitting a multitone signal (multiple narrowband tones). Each narrowband signal is employed to measure a portion of the channel (subcarriers) to obtain the channel response.

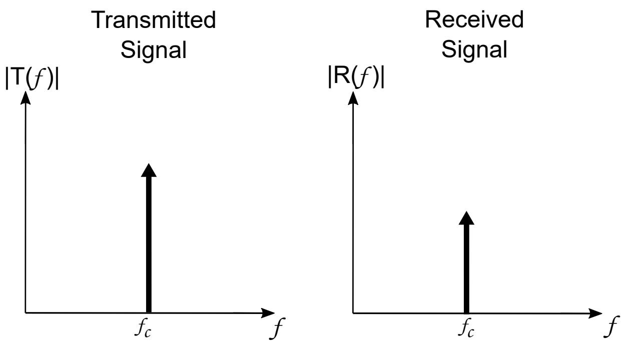

(a) Zero span observation

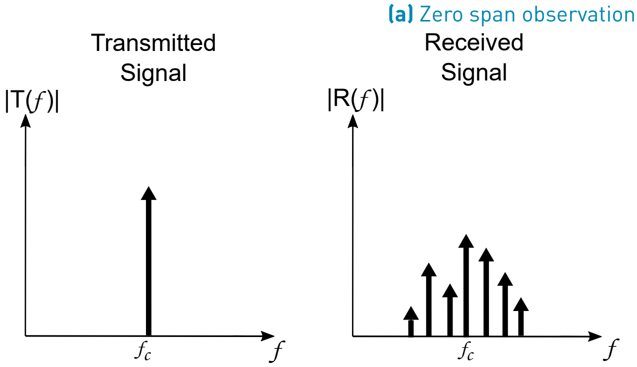

(b) Small window observation

Figure 1 Narrowband channel sounding principle, where $T(f)$ and $R(f)$ denote the transmited and received spectra over frequency f

3. The measurement platform

In this work, the method of narrowband sounding with a small observation window is exploited to construct a measurement platform for the characterization of vehicular channels. The measurement platform is constructed with general purpose RF equipment. This platform allows measuring the DPS of narrowband vehicular channels. To obtain accurate information of the DPS in vehicular environments, the measurement devices must have a short frequency span with an efficient time/frequency resolution to measure fast fluctuations. One of the most encountered problems that are faced

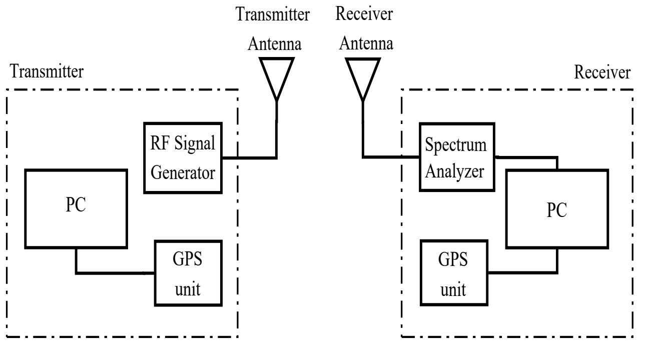

Figure 2 Block diagram of the measurement setup

when using general purpose equipment with no real time processing features, is this trade-off between frequency and time resolution. Therefore, the challenge is to configure a short sweep time considering the largest number of frequency sample points with accurate DPS snapshots. Such a challenge varies from one device to another, but in all cases, the idea is to set the frequency span such that it is about ten times greater than twice the maximum Doppler shift f_{max}. On the other hand, the sampling resolution should be set as small as possible.

A block diagram of the employed measurement platform is depicted in Figure 2. This system consists of a transmitter installed either on a vehicle or on a fixed location depending on whether a V2V or V2I scenario is considered, respectively. On the other hand, the receiver is installed on a vehicle for both V2V or V2I scenarios. The transmitter station comprises a RF signal generator, a half-wavelength dipole antenna, a Global Positioning System (GPS) unit, and a personal computer (PC). Particularly, the Keysight N9310A RF signal generator is employed in this platform. The features of this signal generator enable transmitting a sinusoidal CW at a carrier frequency from 9 kHz to 3 GHz with a maximum power of 20 dBm. For the experimental framework, this station transmits a sinusoidal CW at 760 MHz with 20 dBm of power level. In terms of specifications, the IEEE 802.11p standard specifies a maximum transmitted signal power of 23 dBm for safety applications. On the other hand, the 760 MHz carrier is defined in the ARIB STD-T109 standard as central frequency for DSRC devices. In Mexico, this frequency band is considered for digital television broadcasting. Nevertheless, this frequency spectrum has not been released and it was evaluated in this work through measurements. In this regard, there were not interfering radio signals over the bandwidth of interest. Furthermore, in this station, the PC records its position from the GPS unit.

Table 1 Parameters of the SA for the channel measurement campaign

Parameter	Value
Central frequency	760 MHz
Span	1 kHz
Sample points	601
Sweep time	270 ms
Resolution Bandwidth	5 Hz
Attenuation	0 dB
Pre-amp	ON

On the other hand, the receiver station comprises a spectrum analyzer, a half-wavelength dipole antenna, a GPS unit, and a PC. In our implementation, a Keysight FieldFox N9913A is used as spectrum analyzer. In this device, the parameters were set to obtain an appropriate time/frequency resolution. The configured parameters are summarized in Table 1. The central frequency is located at 760 MHz considering a 1 kHz span to observe the energy spread due to the Doppler effect. This bandwidth is sufficient since the $f_{\max}$ value is around 84 Hz at high speeds (120 km/h) for the 760 MHz carrier. Also, 601 sample points were configured with 6 Hz resolution bandwidth to achieve a balanced sweep time of 270 ms. This sweep time enables to observe the trends and fluctuations of the channel spectrum. In addition, the pre-amplifier of the spectrum analyzer is powered on and a 0 dB attenuation is established. This configuration serves to handle the received signal power. In this station, the PC must capture the DPS and positioning information from the spectrum analyzer and the GPS unit, respectively. Most commercial off-the-shelf spectrum analyzers provide different options to record the measured data. For instance, the data can be stored on an internal memory or on a SD card directly from the device. Nevertheless, in most cases, the information is not stored in a raw format that enables the signal processing on a PC. Therefore, in our implementation the information is captured on the PC using MATLAB, which is achieved by constructing a local network with the spectrum analyzer.

For the experiments, the antennas are placed on the roofs of the vehicles near the front windscreen with vertical polarization. For the V2I channel measurements, the transmitter antenna is settled on the sidewalk on a fixed location. In Section 5, a more detailed description of the positions of the antennas is given.

4. Data reduction for the Doppler statistical analysis

The motion of the mobile stations leads to frequency drifts as a consequence of the Doppler effect. Since the Doppler shift depends on the AOA, the received waves experience different drifts. The contributions of these drifts on the received signal can be observed from the DPS [19].

The Doppler shift experienced by the i-th arriving wave is given as shown in Equation (1):

$$f_i = f_{\max} \cos \alpha_i \tag{1}$$

where α_i is the AOA of the i-th received wave, and $f_{\max}$ denotes the maximum Doppler shift. The maximum Doppler shift $f_{\max}$ is given by Equation (2):

$$f_{\max} = \frac{v}{\lambda_c} \tag{2}$$

where v is the relative speed of the mobile, $\lambda_c = C/f_c$ is the wavelength, with f_c as the carrier frequency, and C the speed of light.
The measured DPS $S(f)$ over a set of discrete frequencies $\mathcal{F}$ (i.e. $f \in \mathcal{F}$) can be characterized statistically by the average Doppler shift and the Doppler spread. The average Doppler shift d_1 is the first central moment of the DPS. It describes the average frequency drift that the signal experiences in the wireless channel. The average Doppler shift is computed from $S(f)$ in Equation (3) [19]:

$$d_1 = \frac{\sum_{f \in \mathcal{F}} f S(f)}{\sum_{f \in \mathcal{F}} S(f)} \tag{3}$$

On the other hand, the Doppler spread d_2 is the square root of the second central moment of the DPS. This quantity describes how the frequency shifts are smeared over the bandwidth. The Doppler spread is related to $S(f)$ as shown in Equation (4) [19]:

$$d_2 = \sqrt{\frac{\sum_{f \in \mathcal{F}} (f - d_1)^2 S(f)}{\sum_{f \in \mathcal{F}} S(f)}} \tag{4}$$

For our purposes, the statistical quantities in Eqs. (3) and (4) must be computed for each time sample. As mentioned on the previous section, a measured snapshot is composed of n frequency sample points $\mathcal{F} = \{f_1, \ldots, f_n\}$ (n = 601 in the presented platform). Therefore, by considering m snapshots of the DPS, the measured information is an $m \times n$ matrix **S**. In other words, each row of the matrix is a measured snapshot of the spectrum analyzer, i.e. a time sample of the DPS. On the other hand, the columns represent the measured frequency bandwidth. To properly compute the statistical moments, the measured data must be linearized from the dBm scale to Watts.

In order to optimize the computation of the Doppler moments, a matrix approach is followed. First, consider the sampled frequency of the form $\mathbf{f} = [f_1, f_2, ..., f_n]$. For instance, the considered bandwidth of 1 kHz will have equidistant values from $f_1 = -500$ Hz to $f_n = 500$ Hz. From the frequency vector **f**, a meshgrid matrix **F** is generated following Equation (5):

$$\mathbf{F} = \mathbf{f} \otimes \mathbf{o} = \begin{bmatrix} f_1 & f_2 & \dots & f_n \\ f_1 & f_2 & \dots & f_n \\ \vdots & \vdots & \ddots & \vdots \\ f_1 & f_2 & \dots & f_n \end{bmatrix} \quad (5)$$

where **o** is an all-ones column vector of length m, and the operator $\otimes$ denotes the Kronecker product.

The meshgrid matrix **F** allows computing a vector that contains the average Doppler shifts (or Doppler spread) by employing element-wise matrix operations directly. The average Doppler shift vector $\mathbf{d}_1$ comprises the values of the mean Doppler shifts for each time sample. Also, the Doppler spread vector $\mathbf{d}_2$ contains the Doppler spread values for each time sample. To compute $\mathbf{d}_1$, first define two auxiliary vectors $\mathbf{s} = [s_1, s_2, ..., s_m]^T$ and $\mathbf{p} = [p_1, p_2, ..., p_m]^T$, where $s_i = \sum_{j=1}^{n} \mathbf{S}_{i,j}$, $p_i = \sum_{j=1}^{n} \mathbf{P}_{i,j}$, and $\mathbf{P} = \mathbf{S} \odot \mathbf{F}$. The notation $\mathbf{A}_{i,j}$ refers to the element in the ith row and jth column of matrix **A**, and $\odot$ denotes the element-wise product. Finally, the average Doppler shift vector $\mathbf{d}_1$ is computed as shown in Equation (6):

$$\mathbf{d}_1 = \mathbf{p} \circ \mathbf{s} \quad (6)$$

where the operator $\circ$ stands for the element-wise division. On the other hand, the Doppler spread vector $\mathbf{d}_2$ is obtained by following a similar procedure based on Equation 4.

5. DPS of vehicular channels

5.1 Measurement scenarios

A measurement campaign of DPS of V2V and V2I communication channels was conducted employing the platform described in the Section 3. For V2V measurements, the RF signal generator (transmitter station) and the spectrum analyzer (receiver station) are mounted on different vehicles. On the other hand, for V2I measurements, the transmitter station is mounted on a fixed location on the street sidewalk.

The measurement campaign was carried out in the city of San Luis Potosí, Mexico, in a location near the main campus of the Universidad Autónoma de San Luis Potosí. This location is an urban scenario composed of a wide street with three lanes in each direction. The same location was considered to conduct the measurements of both V2V and V2I scenarios. Furthermore, this area includes different types of buildings and trees in the roadside. The traffic flow is variable over the day time around this area. Nevertheless, the measurements were performed at an hour with moderate traffic flow.

Figure 3 Considered trajectory for the measurement campaign

The measurements route for this campaign has a length of 1.10 km. This route is shown in Figure 3 as a green solid line, whereas the green marker indicates the position of the fixed antenna used in V2I measurements. For this latter case, the transmitter antenna is located at the sidewalk on a base with a height of 3 m. For the measurements, the receiver vehicle completed the route with an average speed of 60 km/h. On the other hand, for the V2V measurements, both vehicles were moving in the same lane (convoy configuration) with an average speed of 60 km/h and an approximate separation distance of 100 m. In this experiment, the transmitter station was located in front of the receiver station. The average time of the experiments was 70 s recording 100 snapshots of the DPS in each one. The total recording time is influenced by the data transfer time from the spectrum analyzer and the GPS to the PC.

5.2 V2I scenario

The measured V2I channels present a strong LOS component. Figure 4 shows a measured V2I DPS sample for the entire trajectory in a three-dimensional (3D) view. The center frequency is located at 760 MHz with an observation span of 1 kHz, and the observed noise level has an average value of -150 dBm. The signal power is scattered around the central frequency with a trend to the positive side of the frequency band at the beginning of the route, and to the negative side for the second half of the trajectory. This scattered energy is bounded by $\pm f_{\max}$, which for the 60 km/h speed is approximately equal to $f_{\max} \approx 42$ Hz. Nevertheless, these bounds vary slightly due to the velocity variations during the route. For instance, the authors in [13] discuss the non-stationary properties of the vehicular channel due to accelerated motion, i.e. velocity variations. The scattered energy shows the frequency dispersive characteristics of the vehicular channel. In addition, the energy scattering varies over the route, as one can observe from the drift in the high power peaks (red samples). Figure 5 shows the top view of the DPS. In this figure, when the vehicle crosses in front of the antenna, the highest power level has a transition from the positive side of the bandwidth to the negative one. This is explained by noting that, at the beginning of the route, the power peaks are observed in the positive side of the bandwidth as the vehicle starts approaching the transmitter antenna. Therefore, most of the received waves arrive in the front of the vehicle. Then, as the vehicle approaches the transmitting antenna, the power peaks commute to the negative side. The rest of the route, the received waves arrive at the back of the vehicle as it passes over the antenna. The energy is then scattered at the negative side of the bandwidth.

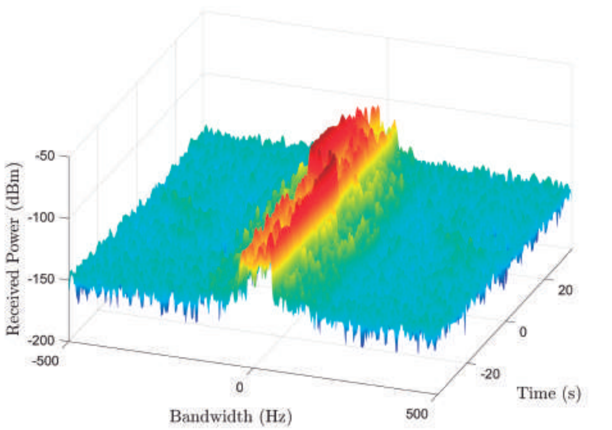

Figure 4 3D view of a DPS sample of V2I communications

To study the frequency dispersion of V2I channels, the statistical moments of the DPS were computed. The measured spectra were averaged over a small signal bandwidth to obtain the moments of this scenario. The results of the statistical moments for this case are shown in Figure 6. The average Doppler shift changes from the positive side to the negative side of the spectrum, which describes the dynamical behavior of the vehicle regarding to the fixed antenna. The average value is close to the $f_{\max}$ and is almost constant in the two defined sections where the vehicle is far from the antenna. Therefore, the frequency dispersion is small in this scenario due to the predominant LOS component. The average value shows magnitude variations due to the changing velocity during the route. On the other hand, the Doppler spread

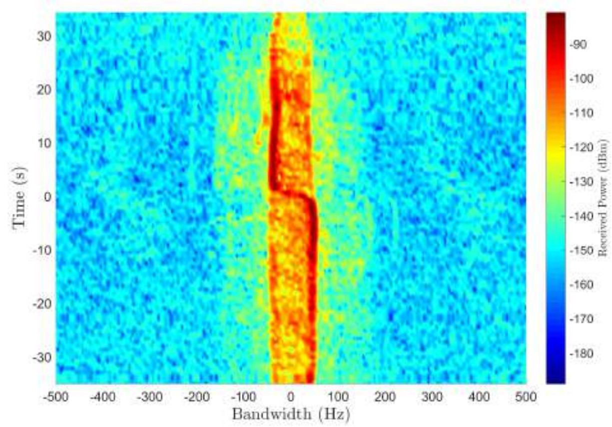

Figure 5 Top view of a DPS sample of V2I communications

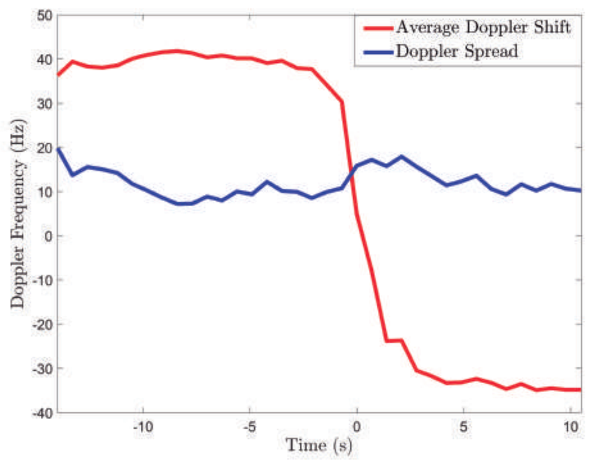

Figure 6 Moments of the DPS of V2I communications

shows an almost constant value, which varies due to the velocity changes during the route. We can conclude that the energy spread is constant over the route.

5.3 V2V scenario

The DPS measurements of V2V scenarios differ from the V2I spectrums above since the energy is scattered over a wider frequency band and the LOS component is observed in the central frequency the entire route. A sample of a V2V DPS for the entire trajectory is shown in Figure 7. The center frequency of this spectrum is located at 760 MHz with a 1 kHz span. The noise level has an average value of -150 dBm. The LOS component presents light Doppler drifts and an almost constant power level during the route. Also, the effects of frequency dispersion can be observed in the form of scattered energy, which is contained on a bounded region (red samples) around the central frequency.

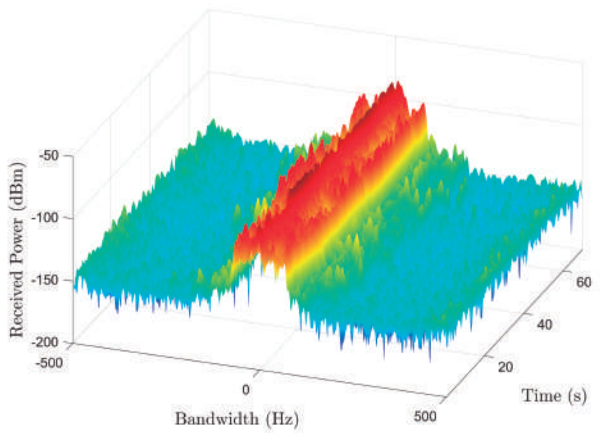

Figure 7 3D view of a DPS sample of V2V communications

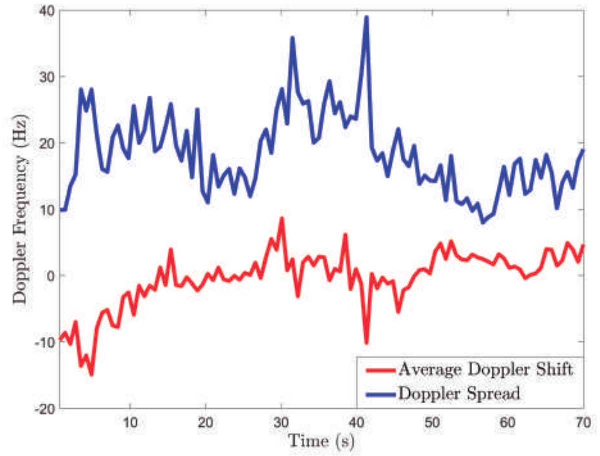

Figure 9 Moments of the DPS of V2V communications

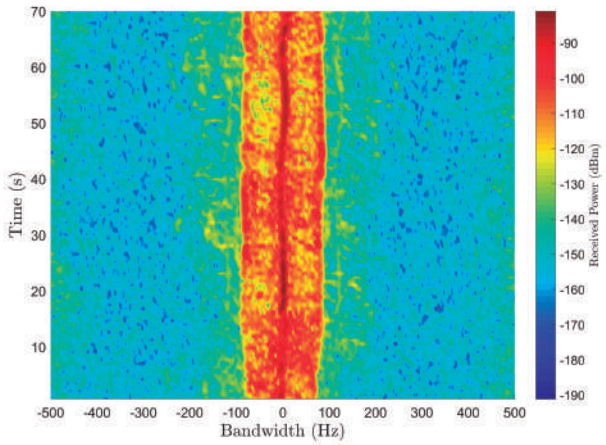

Figure 8 Top view of a DPS sample of V2V communications

To observe the distribution of the scattered energy, Figure 8 shows the spectrum from a top view. This view shows that the energy is scattered in both positive and negative sides with high power levels. This implies that for this V2V scenario, the received waves come from all directions. The high power levels are explained by the fact that the separation distance between vehicles was small. Furthermore, the bounds of the scattered energy varies with time since the speed was not constant during the route as in the previous case. In addition, on the sides of the scattered energy, there are power values that do not correspond to noise levels. These contributions can be scattered energy due to mobile interfering objects (other vehicles on the move).

In order to compute the DPS statistical moments, the measurements were averaged over a small bandwidth. The results of the statistical moments for this trajectory are shown in Figure 9. The magnitude of the average Doppler shift varies between -10 Hz and 5 Hz since most of the received power is concentrated in the LOS component. The computed average value presents high oscillation due to the constant changes in the velocity of the vehicles and the distance between them. On the other hand, the Doppler spread also presented several oscillations due to these conditions.

6. Conclusions

This work presented the implementation of a narrowband sounder for DPS measurements of vehicular radio channels. Since this measurement platform is constructed with general purpose RF equipment, it is easy to replicate. Using this platform, a measurement campaign was conducted to analyze V2V and V2I communication scenarios in the 700 MHz band. The processing and visualization of the collected data allowed analyzing the spectral properties of the vehicular channels.

In the V2I communication case, the Doppler effect influences in a different form the channel whether the vehicle is approaching or moving away from the transmitter antenna. The statistical results show that the signal energy tends to the $\pm f_{\max}$ values in the cases when the mobile is far from the antenna. As the vehicle is closer to the antenna, a different behavior is observed, presenting a transition of the highest power level. Nevertheless, we observed that the Doppler spread is small and almost constant during the route, presenting slight oscillations due to the environmental conditions. On the other hand, for V2V communications, the scattered energy is distributed over a wider frequency band with presence of a strong LOS component. Nonetheless, the energy is concentrated in this LOS component with light Doppler shifts. The statistical results of V2V scenarios present high oscillation due to the LOS component and the traffic conditions. Also, the presence of energy scattered by mobile interfering objects was observed. The results of this measurement campaign show that that narrowband sounding principles can be exploited to study the spectral properties of frequency-dispersive vehicular channels.

In addition, similar experiments can be performed in different propagation scenarios employing the presented platform.

To complement the results presented here, an extensive measurement campaign must be conducted considering different propagation scenarios and other channel characteristics, e.g. the envelope distribution.

7. Acknowledgements

This work was funded in part by the Consejo Nacional de Ciencia y Tecnología (CONACYT) of Mexico with the basic science project #241272.

References

[1] G. Rafiq and *et al.*, "What's new in intelligent transportation systems?: An overview of european projects and initiatives," *IEEE Vehicular Technology Magazine*, vol. 8, no. 4, pp. 45–69, Dec. 2013.

[2] P. Papadimitratos, A. de la Fortelle, K. Evenssen, R. Brignolo, and S. Cosenza, "Vehicular communication systems: Enabling technologies, applications, and future outlook on intelligent transportation."

[3] J. B. Kenney, "Dedicated short-range communications (DSRC) standards in the United States," *Proceedings of the IEEE*, vol. 99, no. 7, pp. 1162–1182, Jul. 2011.

[4] G. Karagiannis and *et al.*, "Vehicular networking: A survey and tutorial on requirements, architectures, challenges, standards and solutions," *IEEE Communications Surveys & Tutorials*, vol. 13, no. 4, pp. 584–616, Fourth 2011.

[5] IEEE 802.11p, *Amendment to Standard for Information Technology-Telecommunications and Information Exchange Between Systems-Local and Metropolitan Area Networks-Specific requirements - Part 11: Wireless LAN Medium Access Control (MAC) and Physical Layer (PHY) Specifications-Amendment 7: Wireless Access in Vehicular Environment*. IEEE, 2010.

[6] ARIB STD-T109, *700 MHz Band Intelligent Transport Systems*. ARIB, 2013.

[7] C. X. Wang, X. Cheng, and D. I. Laurenson, "Vehicle-to-vehicle channel modeling and measurements: Recent advances and future challenges," *IEEE Communications Magazine*, vol. 47, no. 11, pp. 96–103, Nov. 2009.

[8] C. Mecklenbräuker and *et al.*, "Vehicular channel characterization and its implications for wireless system design and performance," *Proceedings of the IEEE*, vol. 99, no. 7, pp. 1189–1212, Jul. 2011.

[9] W. Viriyasitavat, M. Boban, H. M. Tsai, and A. Vasilakos, "Vehicular communications: Survey and challenges of channel and propagation models," *IEEE Vehicular Technology Magazine*, vol. 10, no. 2, pp. 55–66, June 2015.

[10] L. Bernadó, T. Zemen, F. Tufvesson, A. Molisch, and C. F. Mecklenbräuker, "The (in)validity of the WSSUS assumption in vehicular radio channels," in *Proc. of the 23rd IEEE International Symposium on Personal, Indoor, and Mobile Radio Communications (PIMRC'12)*, Sidney, Australia, Sep. 2012, pp. 1757–1762.

[11] L. Bernadó, T. Zemen, F. Tufvesson, A. Molisch, and C. F. Mecklenbräuker, "Delay and doppler spreads of nonstationary vehicular channels for safety-relevant scenarios," *IEEE Transactions on Vehicular Technology*, vol. 63, no. 1, pp. 82–93, Jan. 2014.

[12] C. A. Gutiérrez and *et al.*, "Geometry-based statistical modeling of non-WSSUS mobile-to-mobile rayleigh fading channels," *IEEE Transactions on Vehicular Technology*, vol. 67, no. 1, pp. 362–377, Jan. 2018.

[13] W. Dahech, M. Pätzold, C. A. Gutiérrez, and N. Youssef, "A non-stationary mobile-to-mobile channel model allowing for velocity and trajectory variations of the mobile stations," *IEEE Transactions on Wireless Communications*, vol. 16, no. 3, pp. 1987–2000, March 2017.

[14] T. Abbas and *et al.*, "Simulation and measurement-based vehicle-to-vehicle channel characterization: Accuracy and constraint analysis," *IEEE Transactions on Antennas and Propagation*, vol. 63, no. 7, pp. 3208–3218, July 2015.

[15] L. Cheng, B. Henty, D. D. Stancil, F. Bai, and P. Mudalige, "A fully mobile, GPS enabled, vehicle-to-vehicle measurement platform for characterization of the 5.9 GHz DSRC channel," in *Proc. of the 2007 IEEE Antennas and Propagation Society International Symposium*, June 2007, pp. 2005–2008.

[16] R. Sevlian, C. Chun, I. Tan, A. Bahai, and K. Laberteaux, "Channel characterization for 700 MHz DSRC vehicular communication," *Journal of Electrical and Computer Engineering*, vol. 2010, pp. 1–9, 2010.

[17] H. Fernández, L. Rubio, V. M. Rodrigo, and J. Reig, "Path loss characterization for vehicular communications at 700 MHz and 5.9 GHz under LOS and NLOS conditions," *IEEE Antennas and Wireless Propagation Letters*, vol. 13, pp. 931–934, 2014.

[18] C. A. Gómez-Vega, C. A. Gutiérrez, J. J. Jaime, and J. Vázquez, "Doppler power spectrum measurements of vehicular channels in the 700 mhz band," in *2018 IEEE Colombian Conference on Communications and Computing (COLCOM)*, May 2018, pp. 1–6.

[19] M. Pätzold, *Mobile Radio Channels*, 2nd ed. Chichester, UK: John Wiley and Sons, 2011.

[20] A. Molisch, *Wireless Communications*. Chichester, UK: John Wiley and Sons, 2005.

[21] N. Costa and S. Haykin, *Multiple-Input Multiple-Output Channel Models: Theory and Practice*, 1st ed. John Wiley and Sons, 2010.

[22] A. Molisch, F. Tufvesson, J. Karedal, and C. Mecklenbräuker, "A survey on vehicle-to-vehicle propagation channels," *IEEE Wireless Communications*, vol. 16, no. 6, pp. 12–22, Dec. 2009.